Telmisartan restricts Chikungunya virus infection *in vitro* and *in vivo* through the AT1/ PPAR-γ/MAPKs pathways

Saikat De[1, 2], Prabhudutta Mamidi[1 #], Soumyajit Ghosh[1, 2 #], Supriya Suman Keshry[1, 3], Chandan Mahish[4], Sweta Smita Pani[1], Eshna Laha[1, 2], Amrita Ray[1, 2], Ankita Datey[1, 3], Sanchari Chatterjee[1, 2], Sharad Singh[1, 3], Tathagata Mukherjee[4], Somlata Khamaru[4], Subhasis Chattopadhyay[4]*, Bharat Bhusan Subudhi[5]* and Soma Chattopadhyay[1]*

[1] Institute of Life Sciences, Bhubaneswar, India

[2] Regional Centre for Biotechnology, Faridabad, India

[3] School of Biotechnology, Kalinga Institute of Industrial Technology (KIIT) University, Bhubaneswar, India.

[4] School of Biological Sciences, National Institute of Science Education and Research, HBNI, Bhubaneswar, India

[5] School of Pharmaceutical Sciences, Siksha O Anusandhan Deemed to be University, Bhubaneswar, India

[#] These authors contributed equally to this work

*Address of the Corresponding authors:

Subhasis Chattopadhyay

School of Biological Sciences, National Institute of Science Education and Research (NISER),

Department of Atomic Energy (DAE), HBNI, Bhubaneswar, Jatni, Odisha-752050, India

Phone No: +91-674-2494201; Email: subho@niser.ac.in

Bharat Bhusan Subudhi

School of Pharmaceutical Sciences, Siksha O Anusandhan Deemed to be University

Khandagiri Square, Bhubaneswar, Odisha-751030, India

Phone No: +91-9853945363; Email: bharatbhusans@gmail.com

And

Soma Chattopadhyay

Infectious Disease Biology, Institute of Life Sciences (Autonomous Institute of Department of Biotechnology, Government of India), Nalco Square, Bhubaneswar, Odisha-751023, India

Phone No: +91-674-2304235; Email: sochat.ils@gmail.com

Running Title: Telmisartan regulates CHIKV infection and inflammation

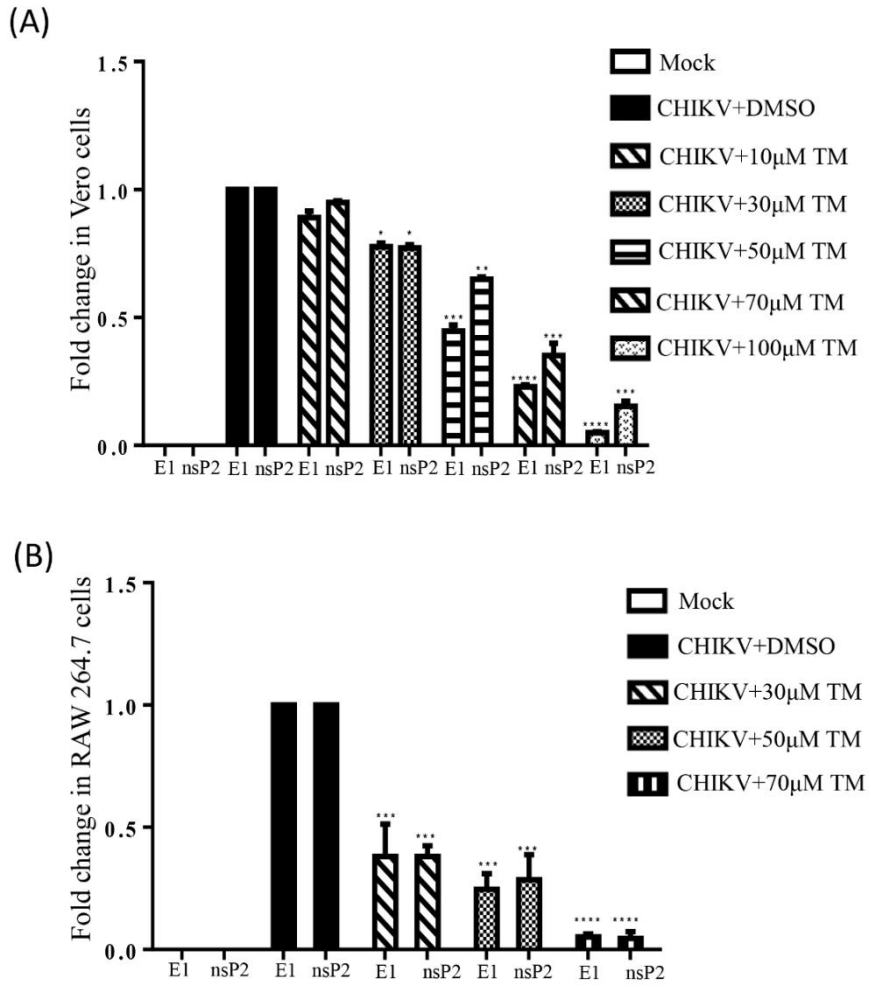

Figure S1. Reduction of CHIKV RNA after TM treatment: Vero cells infected with CHIKV-PS (MOI-0.1) and RAW 264.7 cells infected with CHIKV-IS (MOI-5) were treated with different concentrations of TM and harvested at 18hpi and 8hpi respectively. Whole cell RNA was extracted by TRIzol® and qRT-PCR was performed. (A, B) Bar diagram representing the fold change of E1 and nsP2 genes in CHIKV infected and drug treated Vero and RAW 264.7 cells respectively. Data represented as mean ± SEM (n=3, $p \leq 0.05$ was considered statistically significant).

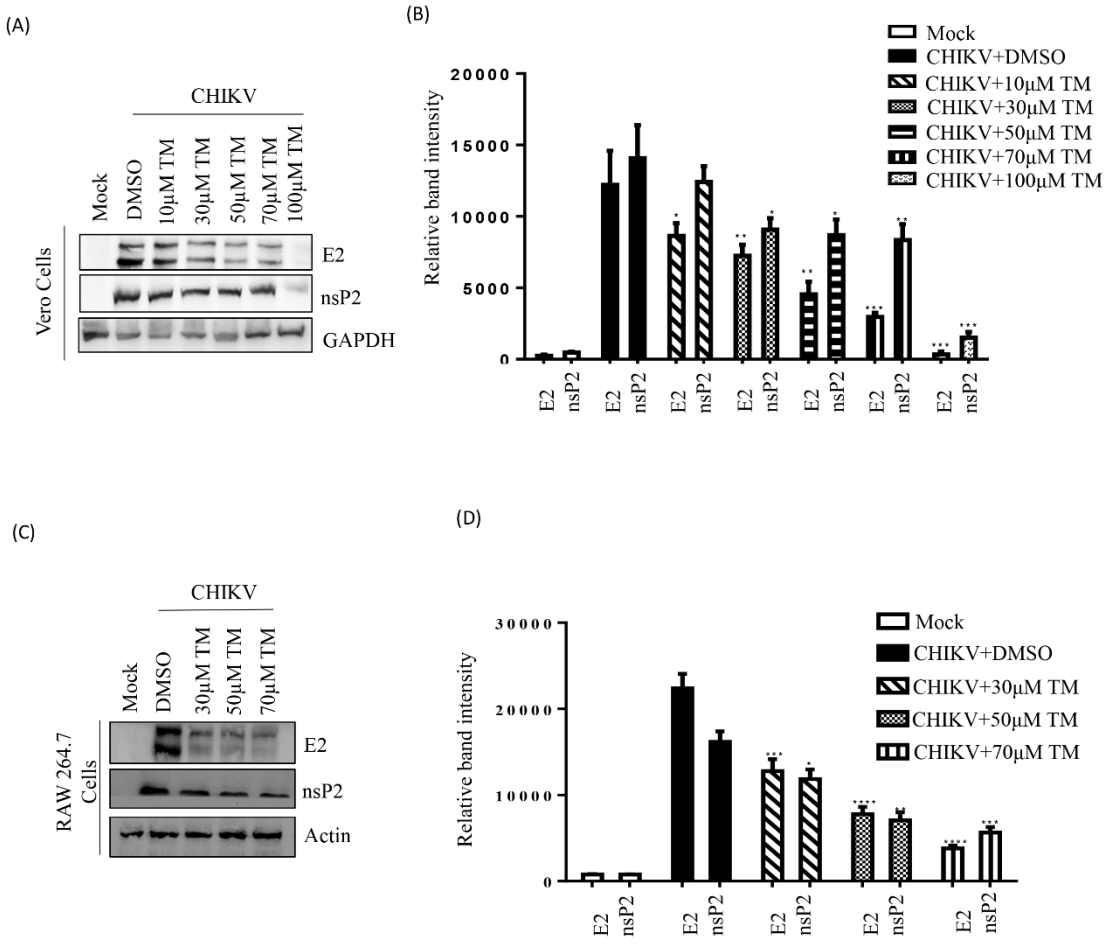

Figure S2. Reduction of CHIKV protein after TM treatment in Western blot: Vero cells and RAW 264.7 cells were infected with CHIKV and treated with different concentrations of TM as mentioned above. Vero Cells were harvested at 18hpi, whereas RAW 264.7 cells were harvested at 8hpi. (A, C) The Vero and RAW 264.7 cell lysates were processed for Western blot using antibodies against CHIKV nsP2 and E2 proteins. GAPDH and Actin was used as a loading control for Vero cells and RAW 264.7 cells respectively. (B, D) Bar diagrams showing the relative band intensities of CHIKV-E2 and CHIKV-nsP2 protein expressions in Vero and RAW 264.7 cells respectively. Data represented as mean ± SEM (n=3, $p \leq 0.05$ was considered statistically significant)

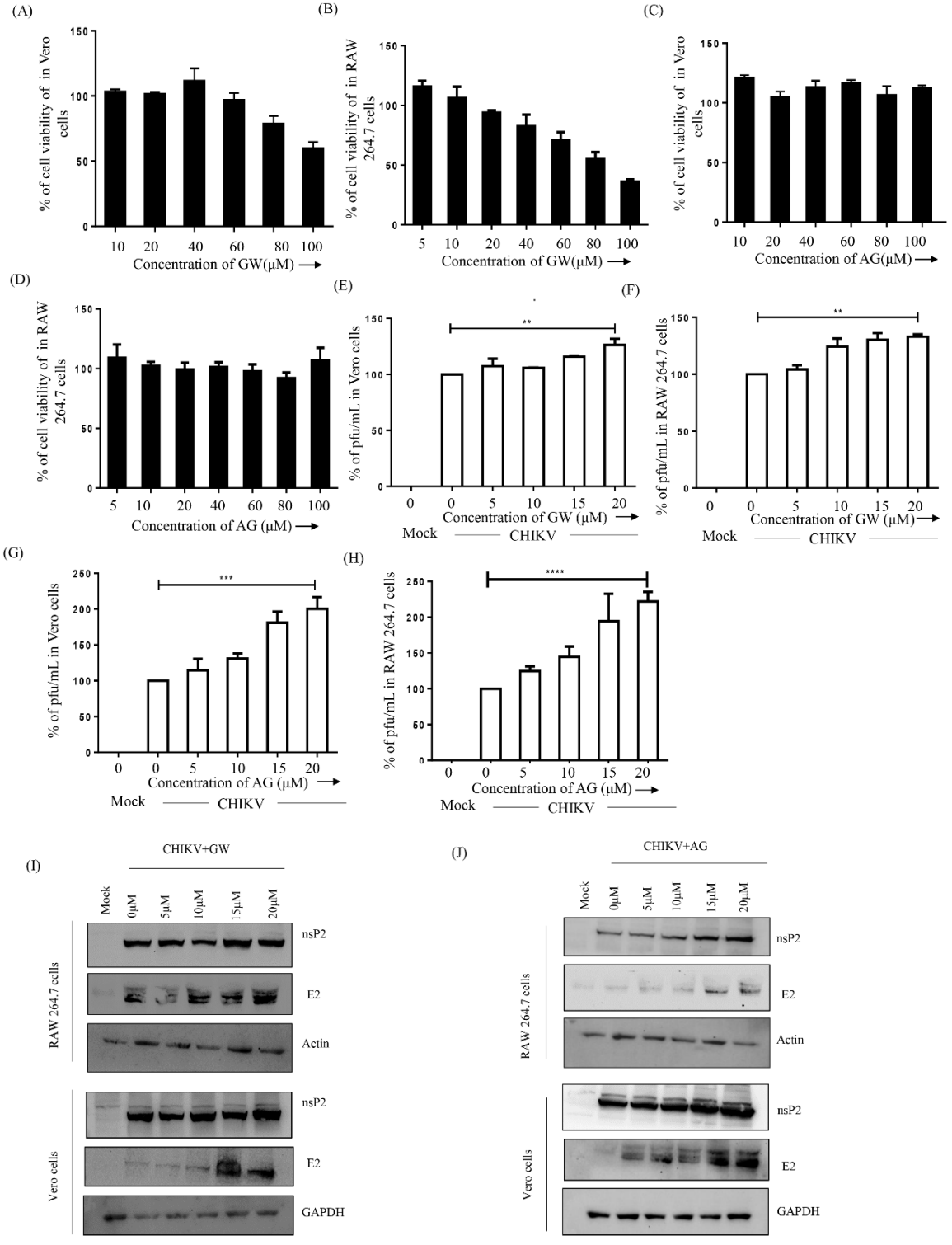

Figure S3. The antagonist of PPAR-γ (GW) and agonist of AT1 (AG) augments CHIKV particle formation dose dependent manner. (A, B**)** Bar diagram shows the viability of Vero and RAW 264.7 in presence of different concentrations of GW. (C, D) Bar diagram showing the viability of Vero and RAW 264.7 cells in presence of different concentrations of AG. Vero cells were infected with CHIKV-PS and RAW 264.7 cells were infected by CHIKV-IS. After

infection GW and AG were added with different concentrations (5µM, 10µM, 15µM, 20µM). The supernatants were collected and virus titers were determined by plaque assay. Cell lysates of the same samples were used for Western Blot. (E, F) Bar diagrams showing the percentage of the viral titer in Vero and RAW 264.7 cells in presence of different concentrations of GW. (G, H) Bar diagrams showing the percentages of the viral titer in Vero and RAW 264.7 cells in presence of different concentrations of AG. Data presented as mean ± SEM. (n=3, $p \leq 0.05$ was considered statistically significant). (I, J) Western Blot showing the expressions patterns of CHIKV non-structural and structural proteins.

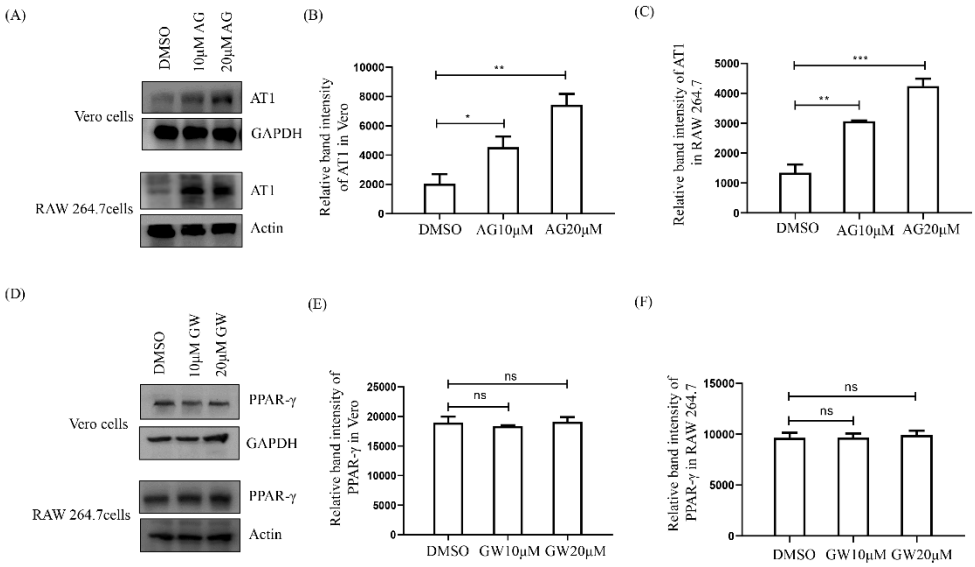

Figure S4. AG upregulates AT1 protein expression, whereas GW has no effect on the protein level of PPAR-γ in both cell lines. Vero and RAW 264.7 cells were treated with different concentrations of AG and GW. Vero Cells were harvested at 18hpi, whereas RAW 264.7 cells were harvested at 8hpi. (A and D) AG and GW treated Vero and RAW 264.7 cell lysates were processed for Western blot using antibodies against AT1 and PPAR-γ proteins. GAPDH and Actin was used as a loading control for Vero and RAW 264.7 cells respectively. (B, C, E, F) Bar diagrams indicating the relative band intensities of AT1 and PPAR-γ proteins expressions in Vero and RAW 264.7 cells in presence of AG and GW respectively. Data represented as mean ± SEM (n=3, $p \leq 0.05$ was considered statistically significant)

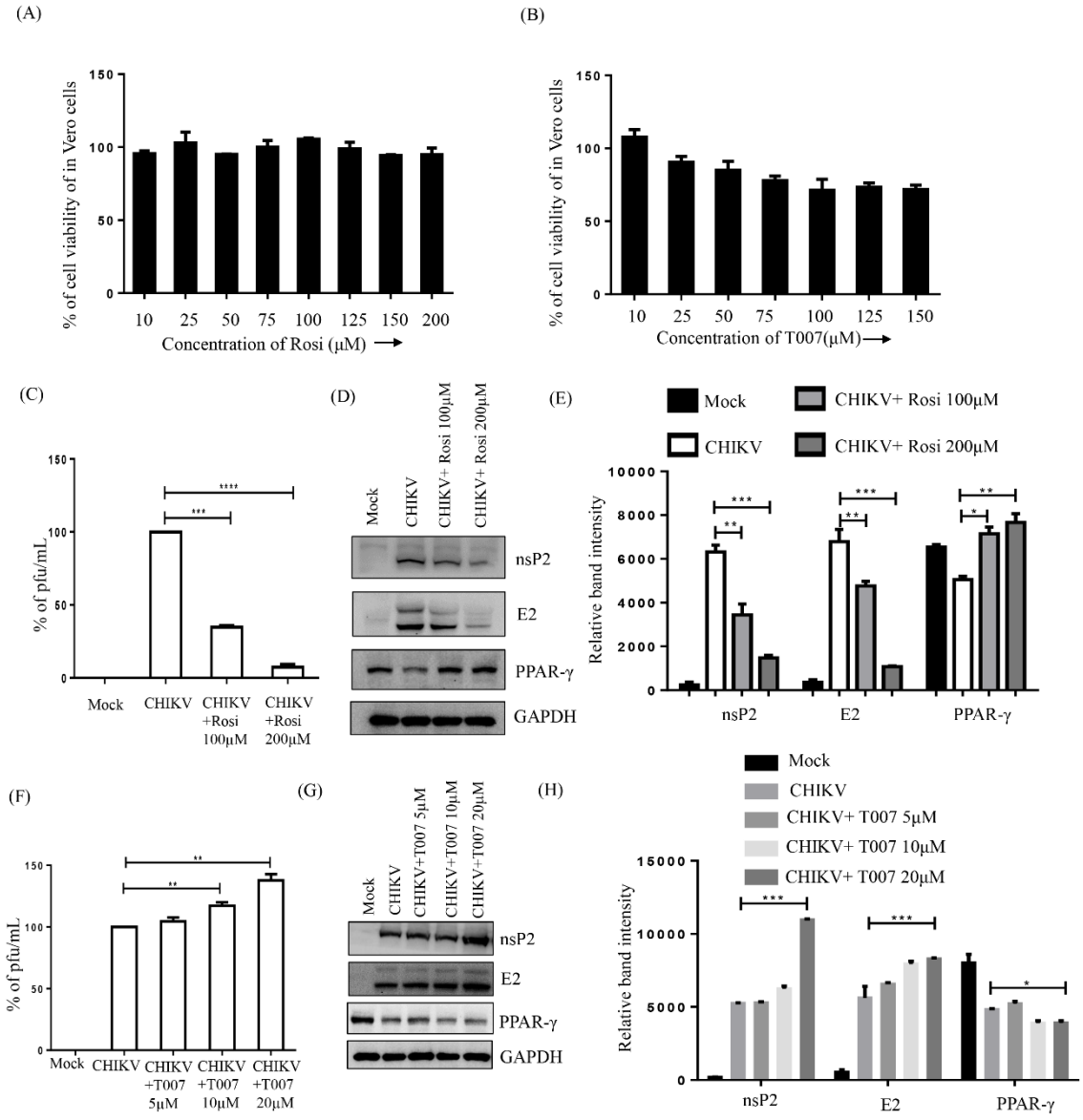

Figure S53. Rosiglitazone (Rosi), the agonist of PPAR-γ, inhibits and T0070907 (T007) the antagonist of PPAR-γ, augments CHIKV particle formation. (A, B) Bar diagrams showing the viability of Vero cells in presence of Rosi and T007. Vero cells were infected by CHIKV-PS at 0.1 MOI and treated with 100 and 200μM of Rosiglitazone (Rosi). Cell supernatants were isolated for plaque assay and Western blot was performed by using the cell lysate. (C) Bar diagrams indicating the percentage of the viral titer in presence of Rosi. (D)

Western blot showing the level of PPAR-γ along with viral nsP2 and E2 proteins after Rosi treatment, where GAPDH was used as loading control. (E) Bar diagram depicting the quantitation of nsP2, E2 and PPAR-γ levels. CHIKV-IS infected Vero cells were treated with 50μM T007 and harvested at 18hpi. Plaque assay was performed by using cell supernatant and Western blot by cell lysate. (F) Bar diagram indicating the percentage of the viral titer in presence of T007 (G) Western blot showing the levels of PPAR-γ along with viral nsP2 and E2 proteins after T007 treatment (5μM, 10μM, 20μM), where GAPDH was used as loading control. (H) Bar diagram depicting the quantitation of nsP2, E2 and PPAR-γ levels after different concentrations of T007 treatment. Data presented as mean ± SEM. (n=3, $p \leq 0.05$ was considered statistically significant).

Table S1: Primer names and sequences.

Sl. No.	Gene	Primer Name	Sequences
1.	Envelope1	CL11F	5’-TGCCGTCACAGTTAAGGACG-3’
2.		CL12R	5’-CCTCGCATGACATGTCCG-3’
3.	nsP2	QNSP2F	5’-GACCCGTGGATAAAGACGCT-3’
4.		QNSP2R	5’-CCCCGCTGTTTCGAGGATAG-3’
5.	Beta-actin	m beta-actinF	5’- AGGCCCAGAGCAAGAGAGGTA-3’
6.		m beta-actinR	5’-ATCTTCTCCATGTCGCAGTGG-3’
7.	GAPDH	GAPDHF	5’-CAAGGTCATCCATGACAACTTTG-3’
8.		GAPDHR	5’-GTCCACCACCCTGTTGCTGTAG-3’